IOP Publishing Journal Title
Journal **XX** (XXXX) XXXXXX https://doi.org/XXXX/XXXX

Transmission Electron Microscopy of the Iron Oxide Core in Ferritin Proteins: Current Status and Future Directions

Surya Narayanan[1], Reza Shahbazian-Yassar[2*], and Tolou Shokuhfar[1*]
[1] Department of Bioengineering, University of Illinois at Chicago
[2] Department of Mechanical and Industrial Engineering, University of Illinois at Chicago
[*]Corresponding author

E-mail: rsyassar@uic.edu; tolou@uic.edu

Received xxxxxx
Accepted for publication xxxxxx
Published xxxxxx

Abstract

Ferritins are an important category of proteins that control the iron storage and release in humans and animals. It is well accepted that various diseases can be traced to ferritin protein abnormalities. In addition, these proteins can revolutionize the field of materials synthesis since they provide an excellent template to grow various nanomaterials with near perfect size and control on chemistry. The ferritin proteins regulate iron ions by biomineralizing or demineralizing various forms of iron oxides. The inner architecture and the microenvironment of ferritin proteins facilitate iron oxide nucleation, enabling the formation of labile ferrihydrite in place of more common iron oxides such as hematite, magnetite, and goethite. The complexity of iron oxide structures and their various stable phases require advanced characterization techniques such as transmission electron microscopy (TEM). This review article summarizes the previous discoveries made by conventional TEM imaging and analytical spectroscopy methods such as electron energy loss spectroscopy and X-ray energy dispersive spectroscopy. With recent innovations in aberration-corrected TEMs, monochromators of electron beams, ultrafast imaging and spectroscopy detectors, integration of Raman within TEM, and 3D tomography techniques, it is now feasible to explore biomineralization within ferritin proteins with an outlook to fully elucidate the signature of diseases that control the nucleation, growth, and stability of iron oxide cores within ferritin proteins.

Keywords: Ferritin, biomineralization, iron oxide phases, aberration corrected TEMs, imaging, spectroscopy

1. Introduction

Ferritins are a family of iron storage proteins that play a significant role in the iron regulation mechanism. The ability of the protein to encapsulate and sequester iron ions highlights its significant contribution towards iron homeostasis in all the living organisms from the lowest to the highest order[1–3]. In the absence of ferritin, low soluble iron in the cells can trigger reactive oxygen species through Fenton's reaction [4]. A typical ferritin protein consists of an outer hollow protein shell, that can accommodate up to 4500 iron atoms within them to form the inner iron core[5]. In humans, the protein shell is made of 24 subunits of light (L-) and heavy (H-) subunit chain amino acids, while prokaryotes such as bacteria and archaea consist of 12 amino acids chain subunits[6]. While H subunits are responsible for iron oxidation, L-subunits are responsible for iron nucleation within ferritin. Despite the differences in the regulation mechanism of prokaryotic and eukaryotic ferritins, the functionality of H- and L- subunits remains the same in all the organisms[1].

The complex architecture as well as the function of the proteins enables synthesis and storage of different materials, highlighting its potential in different applications. Interestingly, the size and crystallographic order of the ferritin core can be related to its the magnetic properties[7]. Yet, the process of iron nucleation is not well understood. Recently, it has been reported that, there is a correlation between the iron misregulation in the brain and neurological disorders[8].While the complex proteins can be utilized to store iron oxides as well as different materials, there is still a lack of knowledge on the causes for iron agglomeration in the brain[7,8].Several light and electron-based microscopy and spectroscopy techniques have been employed to study the structure as well as function of ferritin.

While the light-based characterization techniques can help provide a lot of information about ferritin, it should be noted that these techniques suffer from a diffraction limit of 200 nm[10].As a result, it is challenging to obtain spatial resolution of samples which are less than 200 nm in size. On the other hand, electron-based microscopy and spectroscopy

techniques can provide qualitative information of individual ferritins which are less than 20 nm in size[10].

The shorter wavelength of electrons due to high acceleration voltage and the development of aberration-corrected of the electromagnetic lenses[11], made electron microscopes advantageous to resolve ferritin structure of sub-angstrom resolution[10].Despite this fact, electron microscopes were not made complete use of to study proteins. The need to keep the samples dry before the electrons could transmit through the protein, made the electron microscope's application limited to studying the structure of iron core with severe artifacts[12].

The invention of cryo-electron microscopes (Cryo-EM) requiring the freezing of hydrated protein samples made it convenient to study the structure without drying or causing physical damage to them. However, a low signal to noise ratio was obtained due to vitrified water posed limitations while trying to enhance the contrast of the image without adding negative stain[13]. Also, in order to study the ferritin proteins in dynamic mode, liquid cell based TEM techniques were utilized. Silicon nitride (Si_3N_4) based liquid cells were introduced with an intent to study the structure and function of the proteins in its native state[14].The use of graphene liquid cells electron microscopy (GLC-TEM) improved the spatial resolution[15,16],while maintaining ferritin in its native hydrated state[17]. Further, with a modern aberration corrected TEMs, it is also possible to obtain better spectral information[18,19] that can help tap the chemistry of individual iron atoms within the ferritin proteins[20].

This review article encompasses all the electron-microscopy based studies on ferritin as well as suggests the opportunities that can be utilized to understand the missing knowledge. Since the discovery of ferritin in 1937 [21], there have been several advancements in understanding ferritin proteins. The accomplishments in the field resulted in several review papers with a focus on different aspects of ferritin. The reviews published thus far mainly focused on the structural aspects[22],types of ferritin [23,24],biochemistry aspects[1,25],iron regulation mechanism[26–28], and its implication on human health[28–30], application of ferritin in bionanochemistry[5], and its role as a clinical tool to study the pathological and physiological processes[21].However, until now, there has not been a comprehensive summary on the benefit of utilizing TEM to study the structure and function of ferritins. This review paper aims at addressing this shortcoming and suggests a broader utilization of new advancements in the field of TEM to study ferritin proteins. This paper is designed to provide a basic overview of the structure and function of ferritins. Further, the focus is stirred towards TEM and the description of different techniques involved during the sample preparation for TEM studies. The critical review of the current findings indicates the knowledge related to chemistry, structure, and stable phases of iron oxide core in ferritins. Future studies utilizing techniques such as GLC-TEM, 4D STEM, 3D-electron tomography and integrated Raman system can provide more qualitative information about the iron oxide chemistry in ferritins that should enable a better understanding of ferritin function: the biomineralization and demineralization processes in real-time.

1.1 Structure of Ferritins

The prevalence of ferritin in different life forms prompted researchers to study and identify the structure of ferritin. The existence of complexity in the protein structure emphasizes the need to store and regulate the iron ions, which could otherwise be pernicious to the cytoplasm in the cells. The protein without iron is termed as apoferritin[31].With the total molecular weight of approximately 44 kDa[32], the 24 subunits in apoferritin are assembled by 163 amino acids forming a spherical cavity with outer diameter of 12nm and inner diameter of 7nm[31]. The amino acids predominantly form H- and L- subunits with molecular weight of 21 and 19 kDa. Surprisingly, there is only 55% identity in the two subunit types, resulting in different functions[31]. The ferroxidase (Fe^{2+} binding) sites in H- subunits which facilitate iron oxidation, is absent in L- subunits. As a result, there are differences in the kinetics of iron uptake and release process[4]. The significance of these individual functions of the amino acid subunits is evident, when present in varying ratios in different organs. Vital organs such as the brain and heart consist of ferritins with higher ratios of H- subunits, indicating the need to oxidize the iron ions. On the other hand, organs such as liver and spleen whose primary function is to store iron has ferritins with higher ratios of L- subunits. The ratios of the H- and L- subunits also impact the size of the core as well as kinetics of iron core formation[4]. H- subunits exhibit relatively smaller core and higher rates of iron oxidation as compared to the L- subunits[4].Due to the lack of ferroxidase sites, L subunits take longer time to oxidize iron, yet they can hold more iron ions resulting in a bigger core[4].Recent studies established a relationship between L- and H subunits. It was suggested that L-subunits help enhance the activity of H-subunits, thus favoring the entry of higher number of iron ions in ferritin[33].

While disparity exists in the function of the H- and L-subunits, it should be noted that both H- and L- subunits combine to form a near spherical geometry with a four-fold, three-fold and two-fold axis symmetry, connecting the inner cavity with the outer cytosolic environment (Figure 1(a)) [31]. The amino-acids adjoining the three-fold axis symmetry channel are hydrophilic in nature, comprising of histamine, aspartic and glutamic acid residue[34]. On the other hand, the terminal of four-fold symmetry channels are hydrophobic in nature, with the presence of amino acid residues such as leucine, and glutamine[34].The charges present in the amino acid residues help establish an electrostatic gradient that facilities the entry of iron at the three-fold symmetry channel, as well as exit of iron from the protein via the four-fold channels[35]. Additionally, there are divalent cation binding sites present at the three-fold symmetry which help attach the incoming iron ions to the proteins[34]. However,

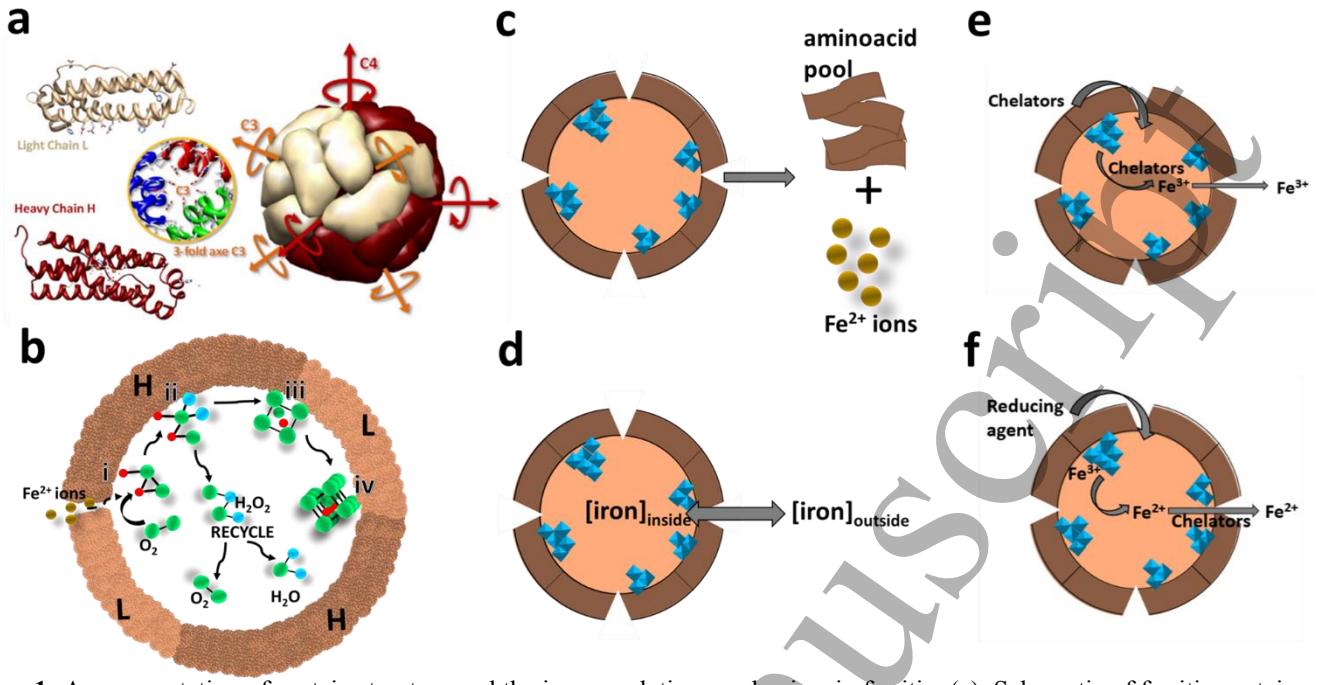

Figure 1: A representation of protein structure and the iron regulation mechanism in ferritin. (a) Schematic of ferritin protein with the three-fold and four-fold channels allowing the entry and exit of iron ions in the proteins (Adapted from Ref.[29]).(b) Biomineralization process in ferritin occurs through a series of steps as shown in (i) Iron oxidation which facilitates the conversion of Fe^{3+} iron species to Fe^{2+} form. An intermediate called μ 1,2 peroxodiferric complex($2Fe^{2+} + O_2 \rightarrow Fe^{3+}$-O-O-$Fe^{3+}$)[134] is formed during this process. (ii) Water reacts with μ 1,2 peroxodiferric complex to recycle hydrogen peroxide: (Fe^{3+}-O-O-Fe^{3+}+$H_2O \rightarrow H_2O_2$+Fe^{3+}-O-Fe^{3+})[134] for the next series of reaction. The (iii) ferrihydrite pre-nucleation clusters formed move towards nucleation site for minerization to form fully grown (iv) ferrrihydrite like crystal. (c) **S**chematic showing the degradation of the protein shell by lysosome which can trigger the iron release.(d)Schematic showing the differences in the concentration of iron within and outside the protein which can trigger iron release.(e) Mechanism of iron removal by direct chelation where iron is released in the form of Fe^{3+} ions which was proved via *in vitro* biochemical experiments.(f) Schematic showing the possible mechanism of iron release by indirect chelation where the reduction of Fe^{3+} to Fe^{2+} ion species is facilitated before iron chelation.

unlike three-fold symmetry channels, there are no binding sites at the four-fold symmetry channels[34]. The intricacy in the structure of the protein not only contributes to the function, but also maintains stability of the protein at extreme physical and chemical conditions such as temperature, pH, and other chemicals[5].This flexibility in the protein structure helped understand the biomineralization and demineralization pathways through several chemistry-based experiments.

1.1 Biomineralization in ferritin

Biomineralization in mammalian ferritin happens through a series of steps led by H- and L- subunits in the protein. The ferroxidase center in the H- subunits consists of four helical bundles of amino acids[31] which initiate the first stage of biomineralization by converting the incoming Fe^{2+} ions to Fe^{3+} form (Figure 1b-i). The conversion of ferrous form to ferric form of iron is facilitated by the oxygen and H_2O_2 present in the buffer solution within the protein[36]. The oxidation of iron can be identified by observing the blue peroxide complexes (λ_{max} ~ 650nm) through UV-Visible spectroscopy measurements[26].The formation of complex reactions can also be verified by Raman spectroscopy, stopped-flow kinetics, Mossbauer spectroscopy, and extended X-ray absorption fine structures (EXAFS)[26].The peroxide complexes are formed as a result of conversion from first formed intermediates to more stable μ-1,2 diferric-peroxo complex (Figure 1b-ii) or differic-oxo/hydro-mineral precursors[36,37]. H_2O_2 is conserved during this reaction, in order to be used for the next set of redox reactions[36].The thus formed diferric-oxo/hydro-mineral precursors (Figure 1b-iii) move towards the interior of the protein, where the nucleation is facilitated by the L- subunits (Figure 1b-iv)[26].At the onset of iron nucleation, the catalytic reactions are translocated to the surface of the already formed iron core[38].This is also supported by the recently published article which suggests that hydrogen peroxide induced oxidation occurs at the beginning of biomineralization, where there are fewer than 500 iron ions in each apoferritin[39]. However, with increase in the iron concentration, the iron ions

deposit directly on the surface of the core where oxidation is favored[39].

The presence of phosphate in the core also dictates the iron binding and accelerates the oxidation processes[40]. Although it was suggested that phosphate bridges the iron core with the apoferritin[41], it was also shown that the absence of phosphate does not prevent the formation of iron core in reconstituted ferritin[42].Meanwhile the source of phosphate was questioned. Experimental evidences showed that inorganic phosphate was adsorbed by the ferritin after the core formation[42].

There was a substantial interest in identifying the iron oxides formed during the initial stages of biomineralization. The results from the electron paramagnetic resonance (EPR) suggested the formation of mononuclear Fe(III) species[43] at the beginning of biomineralization. On the other hand, electron nuclear double resonance (ENDOR) measurements indicated mixed valence species[44] which was also supported by Mossbauer spectroscopy[45,46]and EXAFS[46] results. While the stages of iron nucleation mechanism are still not understood, it should be noted that there are several sites within the protein cavity available for iron binding[43]. Despite this fact, the iron ions selectively bind to the thermodynamically favorable sites which can enable iron core formation[47].

1.2 Demineralization in ferritin

Unlike biomineralization, demineralization in ferritin is sparsely explored. The iron removal process is extremely slow unlike the case in biomineralization. It takes about a year to equilibrate the iron in the human body[36]. With ferritins holding up to 14% of iron in the form of minerals, it might be difficult to remove iron within the timeframe set for the laboratory experiments. In fact, traditional chelators such as deferoxamine, deferiprone, and deferasirox that are used to treat iron overload conditions[48], remove iron at 15 times higher rate as compared to the physiological process[49]. However, the kinetics of iron release can be different when there is immediate need for iron in the body. The pathway for demineralization could be dependent on cellular environment. Due to this fact, understanding the mechanism of iron release in *in vivo* condition has been notoriously difficult.

In a physiological condition, iron release is facilitated when there is low concentration of iron in the cytoplasm. Based on the *in vitro* experiments, it is suggested that the ferroxidase sites in the H- subunit chains do not participate in demineralization process, yet there is a unique way by which iron is released[50].While the iron release mechanism is still questioned, there are four main biochemical models that have been proposed to explain the mechanism of demineralization. The models are:

(a.) *Degradation of the protein by lysosome can cause iron release* (Figure 1c) [51]
(b.) *Diffusion-based iron release triggered when there is concentration gradient between the inner core of proteins and outer cytoplasm*(Figure 1d) [52]
(c.) *Direct chelation of Fe^{3+} ions from ferritin* (Figure 1e) [53].
(d.) *Indirect chelation facilitated by the reduction of Fe^{3+} to Fe^{2+} form and chelation of Fe^{2+} ions* (Figure 1(f)) [54].

Of all the proposed models, iron removal by indirect chelation is the most accepted model. This route of iron removal is supported by the presence of naturally available reducing agents such as ascorbic acids, glutathione, and riboflavins[55]. It is also backed up by the findings of the iron chaperone protein, human poly(rC)-binding protein 1(PCB1) expressed in yeast cells[56]. PCB1, an RNA binding protein in cytosol and nucleus, is present abundantly in mammalian cells. *In vivo* experiments suggested that PCB1 binds directly to the iron core of the protein to facilitate release[56].While this theory is convincing in terms of the ability of PCB1 to prevent free radicals, one should also consider the effects of PCB1 at varied iron concentrations in the cytosol.

Several other theories such as subunit displacement[22], diffusion through gated pores[57], reduction potential that facilitates iron release from the protein shells[58], and diffusion of ions through the channels[59] have been proposed to understand the iron release process. While these theories allow the possibility to explore different pathways, the presence of many different biological cues involved, makes it challenging to understand the process. Advancements in the characterization techniques and ability to detect multiple biological events simultaneously at nanoscale resolution would perhaps help better understand the processes.

2. Ferritin Sample Preparation Techniques for TEM Studies

Like any other biological material, ferritin protein contains water molecule surrounding them. To be able to study the ultrastructure and chemistry via electron microscopy, there is a need to remove the surrounding water, so that electron interaction with the sample can be facilitated[60]. Likewise, biological materials exhibit very poor contrast due to the presence of lighter elements. Despite the fact, it should be noted that the dense iron oxide core in ferritin proteins is visible without staining[22].

2.1. Fix and staining method: The C-TEM sample preparation is designed such that, all the specimen related challenges are taken into consideration. The preparation techniques involve tedious processes that includes chemical fixation with glutaraldehyde (GA) and osmium tetroxide, dehydration, staining, and freeze-drying (as shown in Figure 2(a))[22].The chemical fixation is carried out to preserve the protein

structure, while the other steps are incorporated to make thin sections, increase the contrast, and improve the stability of the proteins[22]. Even though these processes can help image ferritins successfully via TEM as well as scanning electron microscopy (SEM), the observed structures can also produce several visual artifacts. This was evident especially during the heavy metal staining processes which include the usage of uranyl and lead salts[61]. The granular deposits produced by these salts, and also the ability of the salts to penetrate the protein shells defined the morphology of ferritin[22]. On the other hand, the freeze-dried ferritin proteins produced phase granularity as a result of cracks in the metal coating[62]. Not to mention, the thin sectioning of the sample or negative staining also produced artifacts which made it difficult to analyze the iron core of ferritin[22].

2.2. Cryo-EM method: The evolution of Cryo-EM reformed better quality structural information from frozen sample

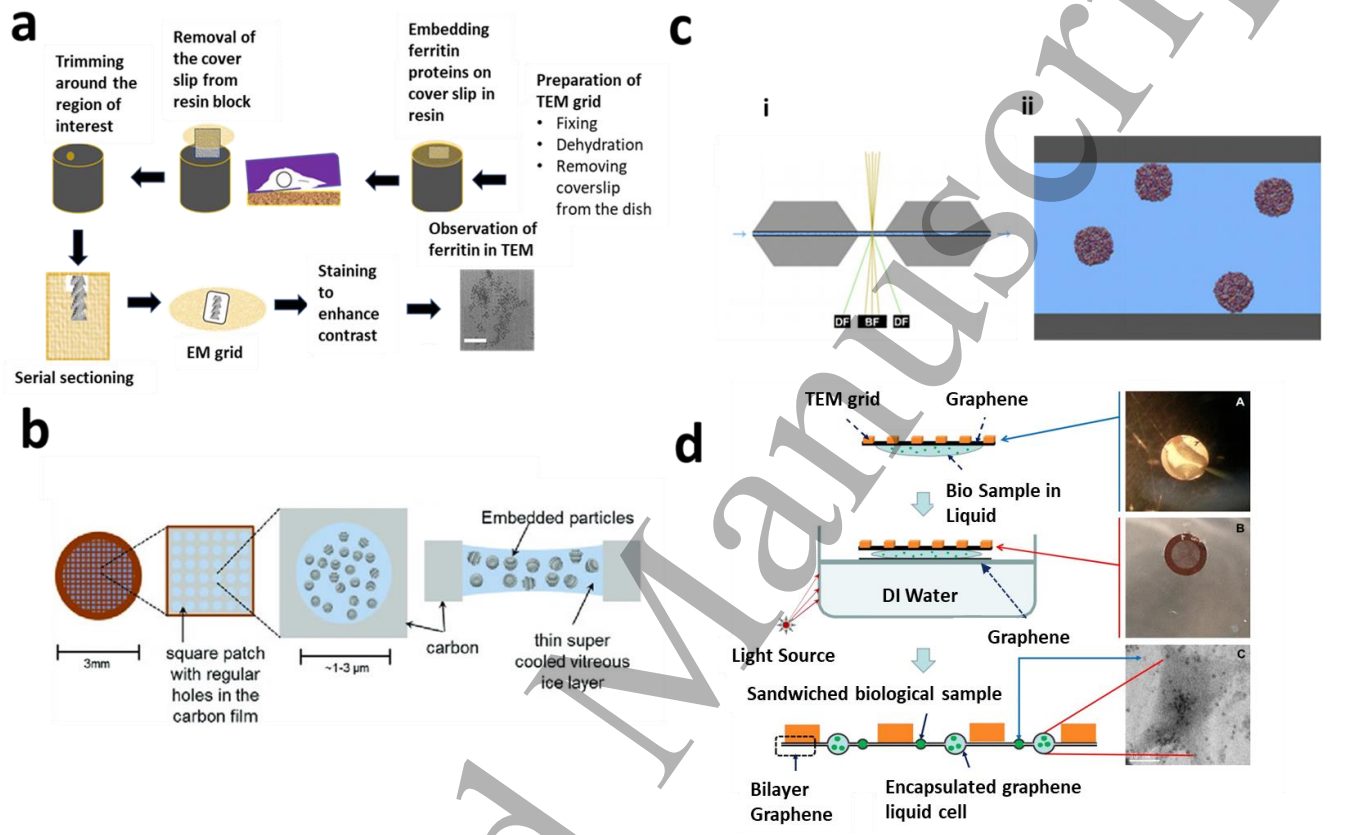

Figure 2: Various TEM sample preparation techniques adapted to study the structure and chemistry of ferritin proteins. (a) Conventional TEM based sample preparation technique which involves series of chemical treatment to fix and stain the ferritin sample. (b) Stages involved during the CryoEM sample preparation (Adapted from Ref.[135]) (c) (i) A schematic that depicts the Si_3N_4 based liquid cell setup with inlet and outlet fluid lines that can enable dynamic as well as static imaging (ii) Visualization of ferritin proteins in liquid state encapsulated within two layers of silicon nitride membrane either found as free floating protein or bound to one of the layers of Si_3N_4 membrane (Adapted from Ref.[14]). (d) Schematic showing the step-wise procedure to synthesize GLCs that can be used to study ferritins in its native liquid state (Adapted from Ref.[17]).

the previous techniques that were used to prepare hydrated biological sample[63].Cryo-EM based sample preparation eliminated the conventional sample preparation steps, while also providing hydration necessary to keep the biological samples wet[63,64]. Typically, Cryo-EM samples are prepared by rapid freezing, such that the surrounding water converts into vitreous ice (Figure 2(b)). It should be noted that the freezing rate of ~10^6 °C/s enables vitreous ice formation instead of crystalline ice[65], thus preventing the occurrence of phase granularity[22].Although it is challenging to observe the protein shell without staining, it is plausible to extract [64,66–68].

Even though Cryo-EM provides opportunities to study the structure of ferritins at high resolutions, there are still challenges, while using this technique: (**1**) specific instrumentation needs during sample preparation and imaging[13]; (**2**) the sample preparation techniques and cooling rates play an important role to preserve the sample from crystalline ice formation. Several experiments and extensive training are required to obtain impeccable results[65]; and (**3**) studying the dynamics of the protein in real-time is challenging considering the short reaction time of different experiments. It should also be considered that

proteins endure in the human body at 37°C, in contrary to Cryo-EM based techniques which require the sample to be maintained at temperatures below -135°C. While the ability of Cryo-EM to retain the native ferritin structure is still debatable, X ray cryo-crystallography results indicated the need for hydration forces to keep the protein stable[69]. In the same work, it was reported that, frozen vitreous ice being inert not only affects the stability, but also interferes with the structural ordering of the proteins[69]. The intercalation of the water molecules with the protein's inner cavity can alter the protein chemistry while increasing the density[70].

2.3. Liquid-cell TEM methods: A growing interest and a need to study the dynamics of biological specimens in real-time enabled the invention of liquid cells-based technique[71].At first, commercially available Si_3N_4 was used to develop spacers and chips which can be placed on top of each other with a minimum distance of 50nm. The biological liquid samples were placed in between the Si_3N_4 membrane[72]. These chips can be accommodated in a specialized fluid cell holder which can also flow liquid through the sample (as shown in Figure(2c-i). This technology helped visualize the dynamics of ferritin molecules for the first time Figure(2c-ii), while maintaining the native surrounding liquid[14,73]. Despite a huge success while imaging biological specimens in liquid, one should also consider the signal-to-noise (SNR) ratio. The ~150-200 nm thick Si_3N_4 liquid cells might compromise the resolution while imaging the ferritin core of diameter ~5-6 nm. In the GLC technique, the Van der Waals interaction between two graphene layers facilitates the wrapping of the biological specimen with surrounding liquid tightly[17]. The thus formed liquid cells help retain the native structure of the ferritin while offering superior spatial resolution[17]. The ease in the sample preparation (Figure 2(d)), and the flexibility offered in imaging the liquid samples with any inexpensive TEM makes it feasible for any kind of experimentation needs. There are different methods adapted in the literature[19], by which GLC samples can be prepared[74]. Direct graphene transfers on the grid[17,18,75] or grid-on-grid sandwich techniques[15,16,76,77] are the most applied techniques to handle biological samples. Nevertheless, considering the size of ferritin protein, using GLC-TEM technique to study protein's structure and function is advantageous over other techniques to obtain qualitative information. With several opportunities and challenges that exist in the sample preparation methods, the nature of the experiment will determine the kind of techniques.

3. Morphological Studies of the Iron Oxide Core in Ferritins

The irregularity in the arrangement of iron oxide crystals during iron nucleation, as well as the number of iron atoms in a given ferritin can influence the formation of core with different crystal structures. Understanding structure of ferritin Although numerous experiments led to the identification of crystallinity of the core (discussed in Section 4), there were core could provide insights on the biomineralization process, as well as serve as a biomarker to draw a comparison between physiological and dysfunctional ferritins.

The structure of the iron core was first considered to be made up of spherical micelles arranged in four different quarters with each micelles measuring about 27Å[78,79].Similar substructures were also observed in ferritins present within the thin ultramicrotomy cell sections[80].Based on the observation of the substructures in the bright field TEM image, and the possibility of random orientation of the core on the carbon film, the core was considered to have fixed number of micelles placed in geometric positions forming a defined pattern[81].Models were constructed based on the substructure of the iron core and it was proposed that there were six micelles arranged sequentially in octahedron shapes[79,82,83].However, these models were not convincing as some of the core structure did not have regular substructures (Figure 3(a))[83] while some of the cores showed more than 6 sub-structural micelles[84].While none of the models could account for the entirety of ferritin core structures, Haydon considered the core substructures to be an effect of artifact produced during the phase contrast and diffraction contrast of the bright field imaging[85].Hayden's experiment was initially questioned[86,87], but later accepted when it was imaged using special support films with low phase granularity[88,89].From the results, it was concluded that ferritin's core is a dense material without any substructures until the evolution of dark field imaging of ferritin core[90].

The dark field imaging mode helped to resolve the structure of the core[91].At electron acceleration voltage of 3 million volts, the granularity of the core began to appear in the images. From those images, it was understood that ferritin mineral core is subdivided into several discrete granular crystal structures[83]. Then the voltage of the microscope was fixed to 50-100kV to avoid the interference of several Bragg's reflection that would appear due to the crystal orientation[22]. The outcome of this work suggested that some of the cores exhibited several small crystallites formed as a result of nucleation of small groups of iron atoms[83].In recent times, STEM imaging offers superior contrast and resolution in the HAADF imaging mode due to the sensitivity to the atomic number (Z-contrast) of the element and the thickness of the sample. The image intensity in HAADF is proportional to the atomic number following: $I \alpha tZ^2$ where I is the intensity from the STEM-HAADF image, t is the thickness of the sample, and Z is the atomic number of the sample[92]. The contrast of the iron oxide core could be improved significantly by imaging human liver ferritins via STEM-HAADF detector through which diffraction contrast could be eliminated[93].

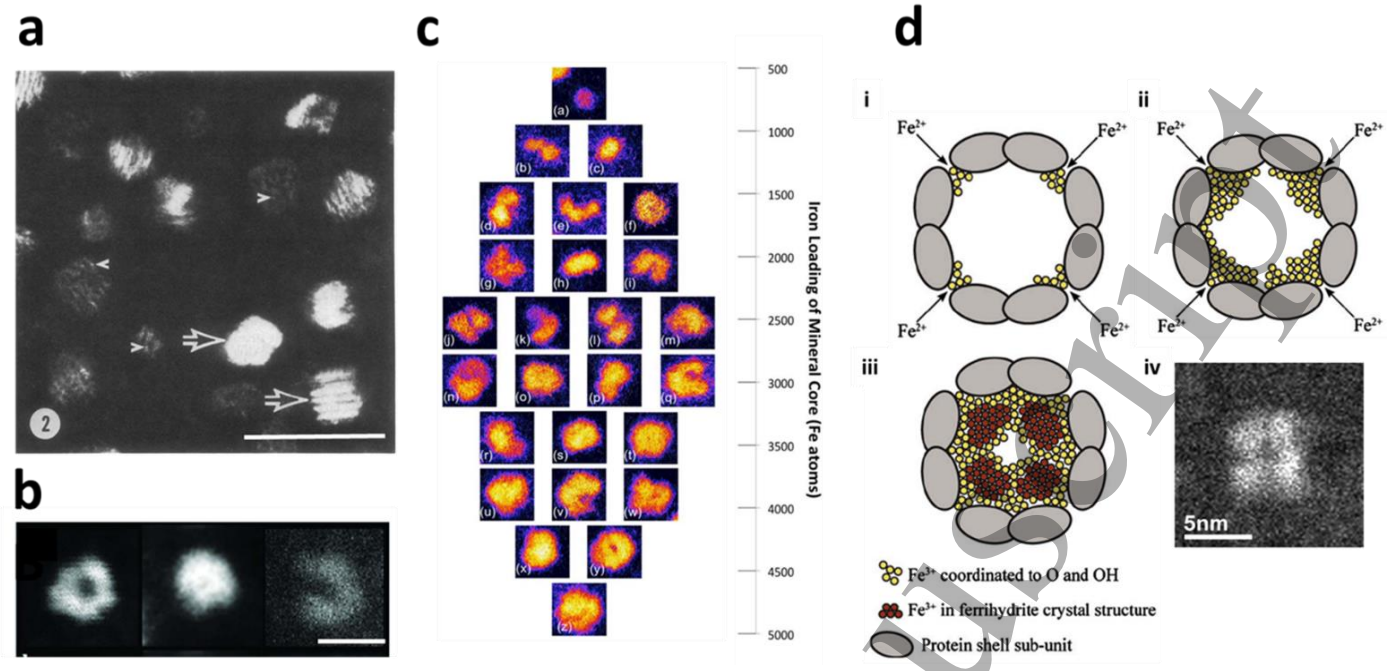

Figure 3: TEM and STEM studies showing different morphologies of iron oxide core in ferritin.(a) Dark-field TEM image of ferritin showing the irregularities that exist in the core structure (Scale:100nm) (Adapted from Ref.[83]) (b) STEM-HAADF image showing the occurrence of different morphologies such as doughnut, spherical and c-shaped substructures(Scale:5nm) (Adapted from Ref.[96]). (c) The different morphologies of the iron core and the corresponding number of iron atoms in each of the morphologies of ferritin via the aberration corrected S/TEM (Adapted from Ref.[98]).(d) A model(figures (i),(ii),and (iii)) explaining the formation of iron core inside the protein shell based on the morphology exhibited in the STEM-HAADF image in figure (iv)(Adapted from Ref.[93]).

still interests in understanding the reason for several small clusters within the protein.

Several possibilities were considered to elucidate the occurrence of substructures in ferritin: (**a**) The protein shell with specific inner architecture provides explicit nucleation sites for the mineral growth. The minerals occupy these sites randomly and grow in any direction[94]. (**b**) The number of nucleation sites and the positioning of the eight hydrophilic three fold channels (channels for the iron entry) determine the morphology[93] while the periodic arrangement of crystals and stacking order can be attributed to the cubic symmetry of the structure[1,95]. This was also supported by 24-n nucleation model, proposed by Lopez-Castro *et al.*[96], which suggests that human spleen ferritin (HSF) encompasses different morphologies because of the higher ratios of L/H subunits, which correspond to the number of nucleation sites in L subunits. On the other hand, with higher ratios of H/L subunits in human heart ferritin (HHF), there are reduced numbers of nucleation sites (n). With 24 subunits that exist in the protein structure, the morphology of the iron core is determined by 24-n subunits available for nucleation of iron (Figure 3(b)). (**c**) The stages of biomineralization and the number of iron atoms present at each stage could contribute to different substructures. This theory was also supported by counting the number of iron atoms present in the iron core via the STEM-HAADF image intensity measurement (Figure 3(c))[97,98]and EELS quantification (discussed in Section 5)[20,93,97].The integrated signal intensity from the HAADF detector is directly proportional to the intensity of the particle given by the equation $N_{intensity} = K.S_{intensity}$,where N denotes to the number of iron atoms and S denotes to the integrated intensity[99]. It should be noted that the assumptions made in these studies consider that the iron oxide core is made of a single crystalline phase ferrihydrite.

The STEM-HAADF could help model (Figure 3(d-i,ii,iii) the mechanism of iron biomineralization based on the morphological evolution of the iron core (Figure 3(d-iv))[93]. It was suggested that iron ions enter the protein through three-fold channels and oxidize at specific sites forming the mineral core. Thus, the formed mineral core is closer to the exit channels. With the protein's capability to absorb more iron ions during biomineralization, the newly entered Fe^{2+} ions oxidize on the surface of the previously formed mineral core. This results in the formation of the iron nucleus prematurely at different nucleation sites. The low thermodynamic stability of the iron nucleus results in very low energy. Consequently, when the protein continues to absorb more Fe^{2+} ions, the previously formed iron nucleus competes for the incoming Fe^{2+} ions, leaving the center of the core hollow. While the proposed mechanism, explains the formation of a morphology observed via the TEM, it does not account for all the morphologies that exist in the protein core. Recently, our group studied the morphologies of HSF and HHF and it was observed that both, HSF and HHF exhibit different

morphologies [134]. While the 24-n model seems logical, it does not help provide detailed explanation for the observed morphologies in HHF. The development in the *in-situ* microscopy and spectroscopy techniques can help explain the occurrence of different morphologies in the future.

4. Crystal Structure/Phase Determination of Ferritin's Iron Core:

Several analyses and models were proposed to understand the structure of the thus formed ferrihydrite core[100–102]. Characterization techniques such as high resolution-TEM (HR-TEM) imaging, microdiffraction[103],and electron diffraction (ED)[104] were employed to validate these models. Of all the models that were proposed in 1960s, Towe and Bradley's work[82], was widely accepted. This model elucidated the structure in terms of lattice constants, iron coordination number, and position of the atoms. From the electron diffraction analysis, it was suggested that the mineral core in ferritin resembles natural mineral ferrihydrite (5 $Fe_2O_3.9H_2O$)[82] with a =5.08Å, and c =9.4 Å. Further, the 4.1 Å and 2.7 Å lattice spacing in the HR-TEM image of human ferritin iron cores (Figure 4(a)) corresponded to (100) and (110) plan of ferrihydrite[105].Although it was proposed that the structure of ferrihydrite resembles hematite (α-Fe_2O_3)[106], it should be noted that hematite exhibited additional diffraction lines at 3.67Å and 2.69Å due to the rhombohedral arrangement of Fe^{3+} ions[107].Moreover, in ferrihydrite structure, Fe^{3+} are in octahedral coordination, placed between 4 oxygen layers spaced 2.35 Å apart[107].

Further, through the *d*-spacings, and lattice orientation obtained from electron microdiffraction studies[108,109],and

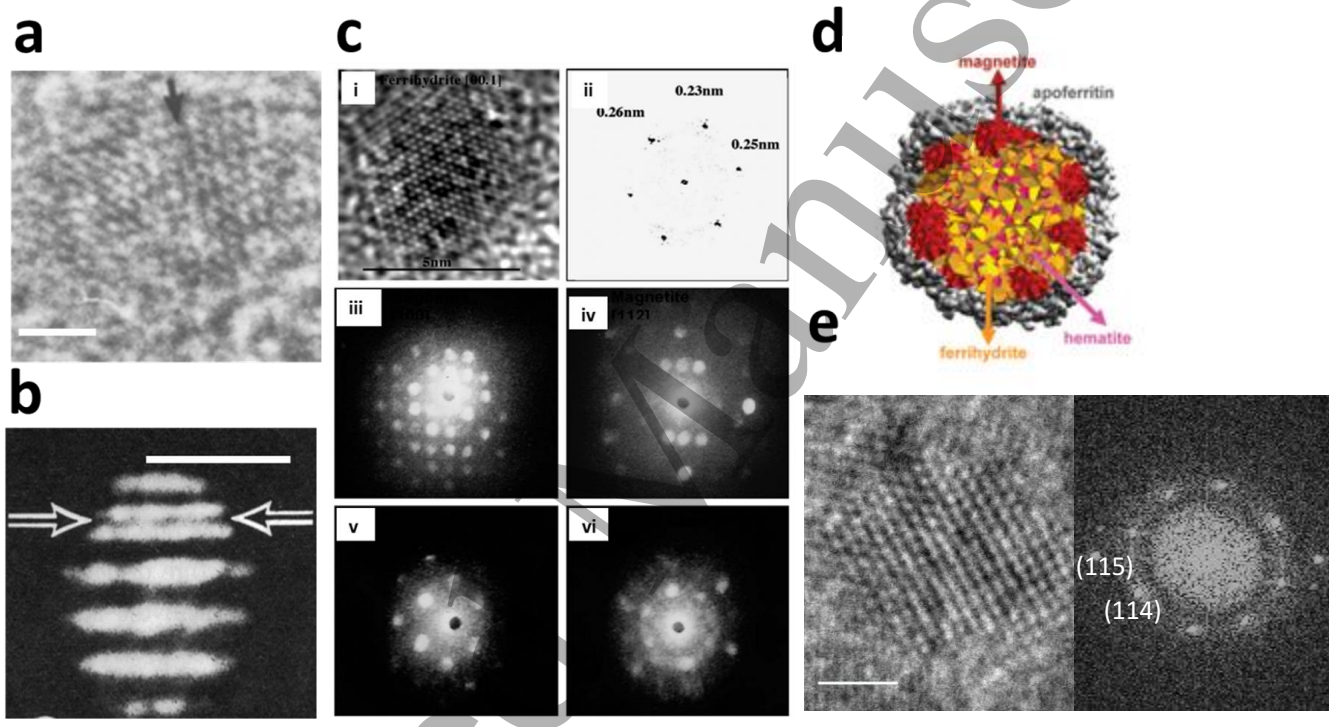

Figure 4: TEM studies to determine the crystallographic information of the iron oxide core in ferritin. (a) HR-TEM image of heat-treated human ferritin with lattice spacings of 4.1 Å and 2.7 Å indicating (100) and (110) planes of ferrihydrite. The arrow in the figure indicates the discontinuity in the lattice plane(Scale:1nm) (Adapted from Ref.[105]). (b) Dark field TEM image of horse spleen ferritin with the arrows indicating the stacking fault in the crystal core structure (Scale:5nm) (Adapted from Ref.[83]). (c) Ferritins extracted from the human brain of the patients who suffered from progressive supranuclear palsy (PSP) and Alzheimer's disease (AD) show (i) the HR-TEM image of the iron core in ferritin, (ii) Fast Fourier transform (FFT) of the core which depicts the crystalline ferrihydrite structure, (iii – vi) Electron nanodiffraction studies of the ferritin extracted from the pathological conditions which indicates (iii) [100] orientation, and (iv) the [112] orientation of magnetite phase. The defects in the crystal structure in (111) planes with a = 4.3 Å are depicted in (v) and (vi) as continuous lines are observed in (v) [100] orientation and (vi) [110] orientation of the face-centered cubic (fcc) plane (Adapted from Ref.[116]). (d) Schematic of the iron core exhibiting the polyphasic nature with different phases of iron oxide in the core (Adapted from Ref.[20]).(e) HR-TEM image and the corresponding FFT of human heart ferritins indicating the presence of (115) and (114) plane of ferrihydrite (Scale: 2nm) (unpublished work).

HR-TEM studies[110] , it was substantiated that the iron oxide core resembled ferrihydrite. However, the HR-STEM image reflected different structures [83,91] unlike all the proposed models[107,111,112].Meanwhile, dark field image also

showed stacking faults (Figure 4(b)) in the crystal structure due to the irregular occupancy of the crystals in certain lattice planes[83]. This observation was also supported by the diffuse diffraction rings[83].It was later observed that the lattice defects in the crystal behave like an interstitial site to deposit phosphate. It should be noted that the iron oxide in ferritin is not completely crystalline. Phosphate dictates the crystallinity of the core[110].With higher ratios of phosphate present in certain invertebrates[110], the iron core exhibits no signs of crystallinity. However, mammalian ferritins have lower percentage of phosphate, which results in crystalline core[110].

The work discussed thus far reported ferritin structure, however the structural-functional relationship was missing. For instance, Towe and Bradley's model[107] suggested that one of the lattice planes represent irregular occupancy of iron. Although this model was widely accepted, one can question the iron uptake and release mechanism with such irregularities in the core structure. Also, one of the biochemical experiments[113] showed biphasic kinetics during the release of iron from ferritin, which supported the Towe and Bradley's model. However, in another study, it was proved that it is possible to reduce Fe^{3+} form of iron to Fe^{2+} form in *ex-situ* condition using a protein called as dihydroflavodoxin[114]. There were questions raised by the scientific community about the composition of the iron core in ferritin, as ferrihydrite belongs to a labile form of iron oxide mineral and a precursor of hematite. The iron core was studied carefully to learn the relationship between Fe^{2+} and Fe^{3+} form. It was then detected that Fe^{2+} and Fe^{3+} iron ions coexist during the iron uptake by ferritins[43,45]. While the significance of studying the function came to light, one of the major turning points was the findings by Quintana and her coworkers[115,116]. They reported that physiological ferritin is composed of different iron oxide phases such as ferrihydrite, hematite, and cubic phases of magnetite (Fe_3O_4)/maghemite(γ-Fe_2O_3) along with stacking faults in the crystal structure (Figure 4(c)). Through HR-TEM and ED, the compositional difference between physiological and pathological ferritin was studied[116].Further through analytical electron microscopy and secondary ion mass spectroscopy (SIMS), the same group reconfirmed the presence of different phases of iron oxides in pathological ferritins[117]. The existence of polyphasic iron oxides (Figure 4(d)) in the core was also supported by Galvez and his coworkers who reported the alterations in the percentage of iron oxide phases during the removal of iron[20]. The presence of different phases of iron oxide was also supported by the HR-TEM and the corresponding FFT, which indicated the presence of magnetite and maghemite[99].

On the other hand, Michel and his coworkers observed a smooth transition from 2-line ferrihydrite to 6-line ferrihydrite during the iron loading process of ferritin from 500 iron atoms to 3000 iron atoms[102]. Based on this total scattering data, they also suggested structural models for the ferrihydrite in ferritin[102]. This study supported the existence of single phase crystalline ferrihydrite form of iron oxide in ferritin. The HRTEM image and the corresponding FFT obtained from the iron core structure of human heart ferritin also exhibited ferrihydrite structure (Figure 4(e)). Since, it is challenging to obtain all the crystallographic planes through HR-S/TEM images, the information obtained through this study was not reliable.

5. Chemical Characterization of Iron Oxide Core in Ferritin

In spite of recent progress in the use of structural characterization techniques such as Mossbauer spectroscopy, EXAFS spectroscopy, and X-ray absorption near edge structure spectroscopy (XANES)[30], these characterization techniques have some limitations to fully resolve the iron oxide core of ferritins. Due to the nanoscale size of iron oxide core, there is need for chemical analysis with high analytical precision and high spatial resolution. Better detectors for X-ray dispersive spectroscopy (EDS) and spectrometers for electron energy loss spectroscopy (EELS) have enabled us to study the chemical signatures at atomic scales[17,75].

Even though both EDS and EELS can be used to study the chemical composition of an element, EELS have an ability to provide fingerprint of the different states of the same element. Further, the benefit of using EDS and EELS compared to other techniques, is their capability to probe individual proteins as against providing a quantitative information[20].While EDS was utilized to identify the presence of iron in the core[117,118], EELS was first used to study the distinction between the iron cores extracted from a healthy brain and the brains affected by progressive supranuclear palpsy (PSP), and Alzheimer's disease[115]. It was found that the iron core of dysfunctional ferritin had higher ratios of Fe^{2+}/Fe^{3+} as compared to physiological ferritin[115]. This study facilitated an understanding of dysfunctional ferritins and its contribution towards neurodegeneration[115].

Further, several groups were inspired to study the energy loss near edge structure (ELNES) of the iron core[93,119]. With the ELNES, one could determine the local structure and the bonding environment within the vicinity of the iron ions. A comparison of ferritin obtained from liver biopsy samples with the synthetic 6-line ferrihydrite(6LFh), elucidated the differences that exist in the chemical composition of both the structures (Figure 5(a))[120]. It was shown that the iron core in ferritin has significantly higher ratios of Fe^{2+} /Fe^{3+}, as compared to synthetic ferrihydrite[120].This study instigated the need to study the redox reactions within the ferritin proteins during mineral formation and disassembly.

Galvez *et al.*[20] were the pioneers to study the chemical compositional changes in ferritin during the process of demineralization by utilizing EELS spectroscopy technique. In this study, they removed the iron from ferritin gradually. The iron oxide phases of ferritin during each stage of demineralization was speculated[20]. It was observed that ferritin with 500 iron atoms had higher ratios of Fe^{2+} /Fe^{3+}, while the fully grown ferritins showed higher ratios of Fe^{3+} /Fe^{2+} [20] . They also showed the differences in the oxidation state in the core and the surface of ferritin (Figure 5(b))[20].

There have been some efforts as well to quantify the

iron oxides in ferritin via the EELS technique (Figure 5(c))[93,97,99]. By using the spectrum imaging technique, the areal density of the atoms (N atoms nm^{-2}) was calculated using the equation: $N = \frac{I_{Fe_{L_{23}}}(\beta,\Delta)}{I_1(\beta,\Delta)\sigma_{Fe_{L_{23}}}(\beta,\Delta)}$ where, $I_{Fe_{L_{23}}}$ is the integral counts under the Fe L_{23} ionization edge, I_1 is the total integral counts of the spectrum in the zero loss and low loss region, $\sigma_{Fe_{L_{23}}}$ is the partial ionization cross section of Fe L_{23} edge obtained after Hartree Slater analysis, β is the collection angle, and Δ is the energy integration window. The addition of the number of iron atoms under each pixel (Figure 5c-ii,iii,iv) helped determine the total number of iron atoms (Figure 5c-v). From this technique, it was suggested that most of the ferritins with fully grown iron core house 2100 $\pm$ 400 iron atoms, while the partially biomineralized ferritin accommodates 320 $\pm$ 60 iron atoms.

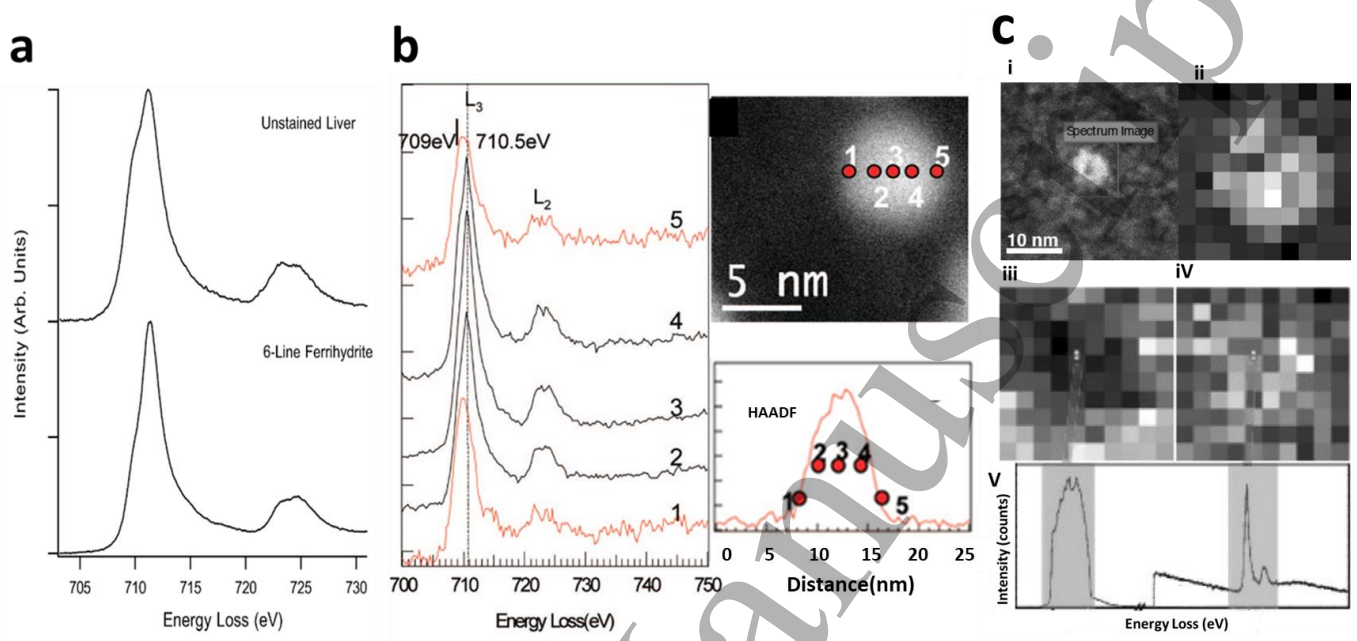

Figure 5: Advancement in EELS spectroscopy to characterize ferritin (a) Comparison of ELNES of ferritin obtained from liver with 6LFh indicated the difference that exist in the iron core structure of ferritin (Adapted from Ref. [120]). (b) EELS spectroscopy acquired from a single ferritin protein indicates the change in the oxidation state while measuring it on the surface and the inner core of the protein (Adapted from Ref.[20]). (c) EELS spectrum mapping (ii) acquired from a human liver ferritin (i) shows the low loss(iii) and the high loss spectrum(iv), and the corresponding signals. This study enables the quantification of iron oxide in ferritin (Adapted from Ref. [97]).

In the first study [121], human liver ferritin (HLF) was compared with 6-line ferrihydrite. It was shown that the electron dose required to reduce iron oxide in ferritin is 100 times lower than electron dose required to reduce the synthetic ferrihydrite[121]. In the same work, they also showed the conversion of substantial amount of octahedral coordinated iron to tetrahedral coordination during excess of electron dose as shown in Figure 6(a). With an accumulated electron dose of 10^6 electrons/nm^2, the reduction of Fe^{3+} to Fe^{2+} ions were observed (Figure 6(b))[121].

In the subsequent studies, through ELNES studies, the same group demonstrated that the influence of electron dose

6. The Effect of Electron Beam

With a possibility of iron transformations that can happen with intense electron dose, one should always consider the prospects of artifacts that can be produced while characterizing the ferritin's iron core crystal structure. Pan *et al* demonstrated the effect of electron dose in ferritin in three independent studies[93,119,121] which suspected that the earlier data presented by Quintana and Cowley[116], and Galvez *et al.*[20], could be an effect of artifacts. The results of Pan and his coworkers suggested that the presence of magnetite and maghemite phases in the core could be a consequence of electron beam facilitated iron transformation which went unnoticed in the former studies.

results in consistent loss of iron coordinating ligands. In this study, they considered Iron phosphate dihydrate ($FePO_4.2H_2O$) and 6LFh as a reference material. Similar to the earlier studies, they showed that the valance state of iron transformed from Fe^{3+} to Fe^{2+} form with increase in electron dose of 3 X 10^6 electrons/$Å^2$ [119]. They could observe the behavior of electron induced beam transformation processes which consisted of two pathways: (1) The direct reduction of octahedrally coordinated Fe^{3+} ions to Fe^{2+} ions; and (2) The conversion of octahedral Fe^{3+} to tetrahedral Fe^{3+} at electron

dose of about 10^6 electrons/nm^2 followed by the change in the valence state of iron with accumulating higher electron doses. However, it was interesting to note that the ratio of Fe^{3+} / Fe^{2+} remained unaltered even with differences in the electron fluence (Figure 6(c))[93,121]. It should also be noted that the current density did not have any contribution in the iron transformations of the core[119].

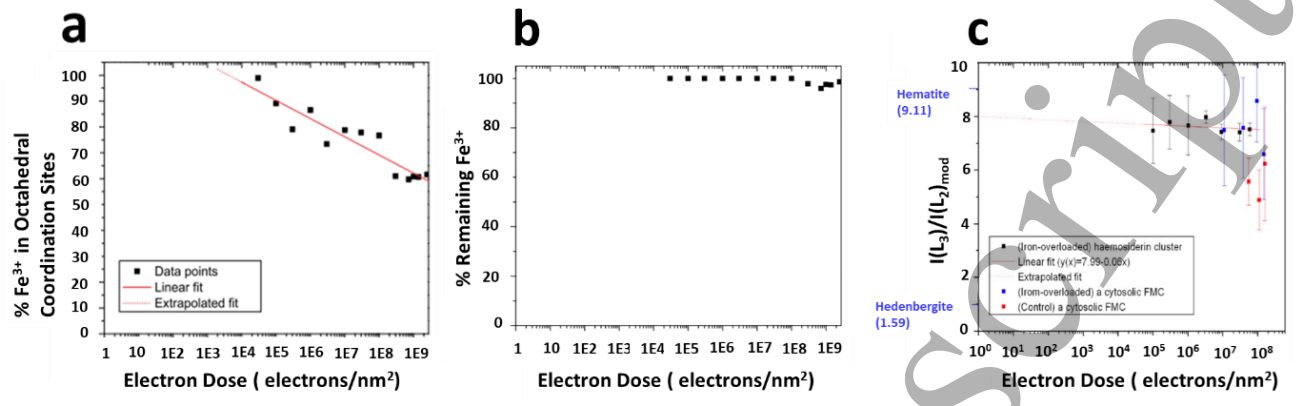

Figure 6: The electron beam induced changes in the iron oxide core of ferritin. (a). Change in the octahedral coordination of Fe^{3+} ions in human liver ferritin due to the increase in the electron dose (Adapted from Ref.[121]). (b) The direct conversion of iron oxides from Fe^{3+} to Fe^{2+} form as a result of increase in the electron dose (Adapted from Ref.[121]).(c) The ratio of integrated areas under L_3 and L_2 edge of iron core of ferritin remains unchanged with the increase in the electron fluence (Adapted from Ref.[119]).

While the effect of electron dose can play a role, the sample preparation techniques are also important. With a protective layer such as GLCs sandwiching the proteins, it is expected that the effect of electron beam induced radiation is mitigated[76]. However, it is still desirable to maintain low electron fluence to prevent the liquid in the GLCs from drying.

7. Future Directions

The progress in microscopy and microanalysis techniques has helped better understand the structure and the function of ferritin. With technical advancements and futuristic work, the possibility of using electron microscopy in a clinical set-up can become reasonable. The section below suggests some of the techniques that can be utilized for better understanding of ferritin proteins.

7.1. Studies of Ferritins in Hydrated State: The conventional TEM based sample preparation techniques involved drying and dehydration of the protein sample, which might introduce artifacts and thus alter the structure. The need to maintain the protein in hydrated state necessitated techniques such as Cryo-electron microscopy (Cryo-EM) and liquid cells. One should note that introducing thick liquid samples in the S/TEM might affect the spatial, and the spectral resolution while imaging the iron core which is less than 10nm in size. This is evident in Cryo-EM[22] as well as Si_3N_4 based liquid cells[14,73]. In two independent studies, James Evans and his coworkers imaged ferritins via *in-situ* liquid cell electron microscopy[14]and dynamic liquid cell TEM[73]. While the spatial resolution reported was not enough to observe the lattice spacings of the iron oxides in ferritin, it should also be noted that there are no studies thus far that report the EELS based chemical analysis of ferritin in Cryo-EM or Si3N4 based liquid cells.

The invent of graphene liquid cells (GLCs) (Figure 7(a)-i) revolutionized the technique of studying the chemistry of ferritin with utmost resolution (Figure 7(a)-ii) while maintaining the native liquid state[17]. GLCs were developed to address the challenges faced by the community while studying biological specimens via the Si_3N_4 based liquid cells[122]. Unlike Si_3N_4 based chips, the GLCs are composed of few layers of graphene with the total thickness of ~1nm, making it more electron transparent[122]. Further, the ability of graphene to conduct and scavenge the incoming electrons plays a prominent role in controlling the electron beam induced damage[76]. Despite the fact, there are several shortcomings with GLC-TEM technology: (**1**) The inherent nature of graphene to hermetically seal the liquid pockets without controlling the liquid thickness makes it challenging to transfer the technical advancements achieved while fabricating Si_3N_4 liquid cells[76]; and (**2**) The success in liquid encapsulation depends on the techniques adapted to prepare GLCs[74], as well as the specimens involved in the preparation[76].

The GLC-TEM helped protect the integrity of the protein samples while imaging, and spectral acquisition as shown

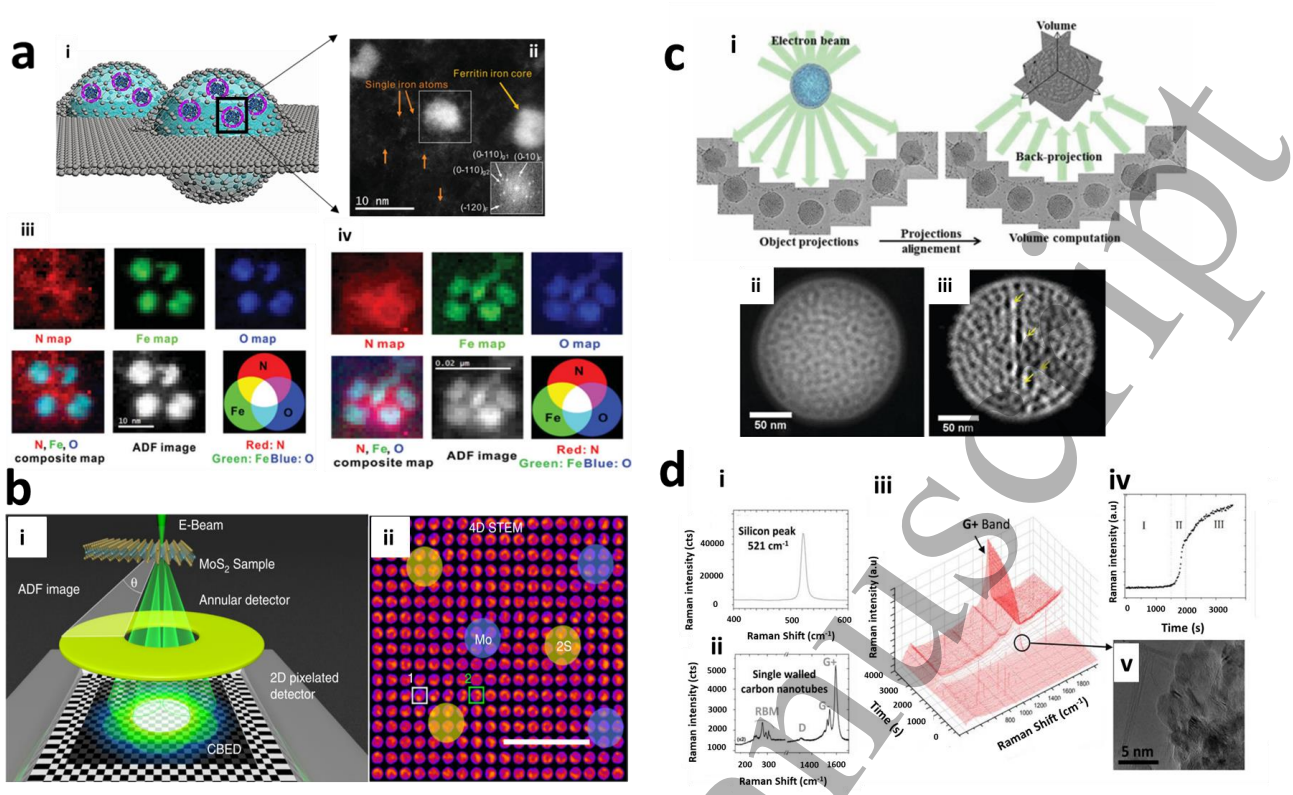

Figure 7: Future TEM directions for the studies of ferritins: (a) Liquid cell-TEM imaging and spectroscopy studies of ferritins: (i) schematic showing ferritins encapsulated in GLCs; (ii) atomic resolution image of the iron core in ferritin via GLC-TEM (Adapted from Ref.[17]); (iii) EELS mapping of ferritin in (ii) dry and (iv) liquid state showing the integrity of proteins in GLCs (Adapted from Ref.[17]).(b) Schematic showing 4D-STEM setup with the CBED image that can be recorded to obtain 4D STEM image; (ii) indicates the capability to determine the atomic composition of the MoS_2 and WS_2 material (Adapted from Ref[125]); (c) Schematic showing (i) 3D electron tomography technique which can be utilized to study crystal defects such as grain boundaries, dislocations and point defect at atomic resolution; (ii) HAADF-STEM image of SiO2-ZrO2 oxide nanoparticles extracted from tilt series that were used to 3D reconstruction of the image; (iii) Cross section through the Z-sensitive volumes can help determine the atomic composition of the material(Adapted from Ref.[128]); (d) Integrated Raman spectroscopy and electron microscopy setup which can be utilized to study the biomineralization in ferritin and protein's conformational changes (Adapted from Ref.[133]).

in Figure 7(a-iii,iv)[17]. (Figure 7a- iii) represents the EELS-mapping of ferritin acquired via conventional S/TEM while (Figure 7a-iv) represents the ferritin imaging via GLC-S/TEM technique. From the nitrogen maps, it can be observed that the structure of the protein is retained when imaged in liquid. Further, in the same work, the structural changes in iron oxide core while measuring it in liquid versus dry state was reported[17].Recently, our group studied the chemical compositional changes in the H and L rich ferritin via the GLC-TEM [136]. The future is promising with the ability to study the time-course assembly and disassembly of iron core in ferritin via the GLC-TEM and monitoring the chemical compositional changes via techniques such as EELS and EDS that can provide qualitative information.

7.2. *Studies of 4D-STEM on Ferritins:* Phase contrast imaging such as STEM is a powerful technique to study the weak phases in any biological material such as ferritin. The ability to control the electron radiation, while being able to record incoherent signals[123] has been a great advantage to study the morphology as well as the crystal structure in ferritin. Despite the advancements, there is still ambiguity while identifying the crystallinity of the iron core in ferritin. The complexity and chemistry that are confined to the local biological environment play an important role in determining the iron oxides. Advancements in STEM imaging techniques such as 4D STEM can possibly identify the localized chemical information by integrating with convergent electron beam diffraction patterns (CBED) that are available during scattering events (Figure 7b-i)[124][125].

The data acquired via the traditional STEM imaging is confined to 2-D datasets with spatial information, while the structural and chemical spectroscopy techniques such as electron diffraction, EDS, and EELS contribute to the 3-D datasets[126]. The ability to combine spatial resolution along with spectral or diffraction information during each STEM

acquisition can improve the Z-contrast imaging along with the analytical signals (Figure 7b-ii). Further, aberration corrected S/TEM can be made use of, to focus the probe below Å scale[126]. Although,4D STEM has the above-mentioned advantages, there is still a need to improve the raster scanning rates and frameworks to store large datasets[126]. Above all, there is a need for faster cameras to record the biological events that occur within few seconds[123].With the progress and developments in this field, it should be realistic to identify the local atomic configuration of ferritin's iron core via the 4D STEM.

7.3. *3D Atomic-Resolution Electron Tomography of Ferritin:* Studying the atomic structure and morphology of the iron core in ferritin could reveal many details such as atomic composition, bonding properties of the material, stacking faults, and iron nucleation mechanism in ferritin. Although the knowledge one could gain from atomic structural studies is alluring, the information gained from traditional aberration corrected S/TEM is limited to observing 2-D structures[127]. Single-particle CryoEM was developed with an intent to study the 3-D structure of biological materials, however this technique can only be applied to study materials with similar atomic configuration[127]. This is a major setback while studying the iron cores of different ferritins which can have random morphologies and atomic configurations.

With STEM-based tomography, it is plausible to study the 3-D structure of ferritin's iron core, while evading the diffraction and the phase contrast produced by any biological sample. The rotation of the sample along the tilt axis helps produce a 2D image at different tilt angles, which is further processed to produce a 3-D image (Figure 7(c-i)). Further, with 3D reconstruction of the HAADF-STEM image (Figure 7 (c-ii)), it is possible to determine the atomic composition based on the Z contrast (Figure 7(c-iii))[128]. It should be noted that, the morphology of the sample plays an important role to provide qualitative information during this procedure[127]. While most of the samples can be tilted only up to $\pm$ 79°, one can tilt the sample with 360° of rotation with needle shaped specimens[129].

Along with the features that 3-D electron tomography offers, one should also consider the sample preparation techniques. An intense electron beam can cause structural changes in the protein shell as well as iron transformations in the core of the ferritin. A combination of low voltage techniques and encapsulation of the ferritin proteins in GLCs could help mitigate the radiation damage, while building the 3-D atomic structures[130].

7.4. *Studies of Simultaneous in-situ Raman and TEM on Ferritins:* The process of biomineralization and demineralization in ferritin is more than a series of chemical reactions. The unique phases of iron oxide crystal core formed in ferritin, as well as protein's role in the mechanism of iron nucleation remains unfolded. It is interesting to observe that the protein shell not only behaves as an iron reservoir but also dictates the type of iron oxide minerals formed[131].In the absence of protein, the iron transformations are meant to occur in a different way. The formation of goethite (FeOOH) phase is more pronounced as compared to the ferrihydrite and hematite phase[131].

While the variation in the mineral phases exists in different organ ferritin, it would be interesting to study the protein structural changes and its contribution towards biomineralization. Also, some of bacterial ferritins are known to exhibit conformational changes during the biomineralization and demineralization process[132].A combination of light-based Raman spectroscopy *and in situ* electron microscopy (Figure 7(d))[133] can help observe the conformational changes in the protein structure while also probing individual proteins to study the chemistry. The correlative technique can improve the quality of information one can obtain through liquid microscopy studies as it can help better understand the structural-functional relationship. Further implementing a less expensive light-based spectroscopy device along with aberration corrected electron microscopy can help identify biomarkers during pathological conditions. With machine learning, one can train the inexpensive device to be able to recognize the biomarkers in a clinical set-up.

Acknowledgments

TS acknowledges funding from NSF career award (DMR-1564950). RSY acknowledges funding from NSF grant DMR-1710049. The authors are indebted to Nasim Farajpour from UIC for her illustration.

References

[1] Harrison PM A P 1996 The ferritins: molecular properties, iron storage function and cellular regulation. *Biochim Biophys Acta ;* **1275:161-2**

[2] Andrews S C, Robinson A K and Rodríguez-Quiñones F 2003 Bacterial iron homeostasis *FEMS Microbiol. Rev.* **27** 215–37

[3] Fischer C J, Yao H, Weeratunga S K, Lovell S, Gee C E, Battaile K P and Rivera M 2010 Structural Studies of Bacterioferritin B from Pseudomonas aeruginosa Suggest a Gating Mechanism for Iron Uptake via the Ferroxidase Center, *Biochemistry* **49** 1160–75

[4] Mehlenbacher M, Poli M, Arosio P, Santambrogio P, Levi S, Chasteen N D and Bou-Abdallah F 2017 Iron Oxidation and Core Formation in Recombinant Heteropolymeric Human Ferritins *Biochemistry* **56** 3900–12

[5] Jutz G, Van Rijn P, Santos Miranda B and Böker A 2015 Ferritin: A versatile building block for bionanotechnology *Chem. Rev.* **115** 1653–701

[6] Bevers L E and Theil E C 2011 Maxi- and mini-ferritins: minerals and protein nanocages. *Prog. Mol. Subcell. Biol.* **52** 29–47

[7] Papaefthymiou G C 2010 The Mössbauer and magnetic properties of ferritin cores *Biochim. Biophys. Acta - Gen. Subj.* **1800** 886–97

[8] Ke Y and Qian Z M 2003 Iron misregulation in the brain: A primary cause of neurodegenerative

disorders *Lancet Neurol.* **2** 246–53

[9] Maher B A, Ahmed I A M, Karloukovski V, MacLaren D A, Foulds P G, Allsop D, Mann D M A, Torres-Jardón R and Calderon-Garciduenas L 2016 Magnetite pollution nanoparticles in the human brain *Proc. Natl. Acad. Sci.* **113** 10797–801

[10] Chen X, Zheng B and Liu H 2011 Optical and digital microscopic imaging techniques and applications in pathology *Anal. Cell. Pathol.* **34** 5–18

[11] Rose H H 2008 Optics of high-performance electron microscopes. *Sci. Technol. Adv. Mater.* **9** 014107

[12] Robertson J D 2013 The Nature and Limitations of Electron Microscopic Methods in Biology *Membrane Physiology* (Boston, MA: Springer US) pp 61–93

[13] He K, Shokuhfar T and Shahbazian-Yassar R 2019 Imaging of soft materials using in situ liquid-cell transmission electron microscopy *J. Phys. Condens. Matter* **31** 103001

[14] Evans J E, Jungjohann K L, Wong P C K, Chiu P L, Dutrow G H, Arslan I and Browning N D 2012 Visualizing macromolecular complexes with in situ liquid scanning transmission electron microscopy *Micron* **43** 1085–90

[15] Firlar E, Ouy M, Covnot L, Xing Y, Lee D, Chan A, He Y, Song B, Afelik S, Wang Y, Shahbazian-Yassar R, Oberholzer J and Shokuhfar T 2019 In situ graphene liquid cell-transmission electron microscopy study of insulin secretion in pancreatic islet cells *Int. J. Nanomedicine* **Volume 14** 371–82

[16] Firlar E, Ouy M, Bogdanowicz A, Covnot L, Song B, Nadkarni Y, Shahbazian-Yassar R and Shokuhfar T 2019 Investigation of the magnetosome biomineralization in magnetotactic bacteria using graphene liquid cell-transmission electron microscopy *Nanoscale* **11** 698–705

[17] Wang C, Qiao Q, Shokuhfar T and Klie R F 2014 High-resolution electron microscopy and spectroscopy of ferritin in biocompatible graphene liquid cells and graphene sandwiches *Adv. Mater.* **26** 3410–4

[18] Ghodsi S M, Anand S, Shahbazian-Yassar R, Shokuhfar T and Megaridis C M 2019 In-Situ Study of Molecular Structure of Water and Ice Entrapped in Graphene Nanovessels *ACS Nano* acsnano.9b00914

[19] Ghodsi S M, Megaridis C M, Shahbazian-Yassar R and Shokuhfar T 2019 Advances in Graphene-Based Liquid Cell Electron Microscopy: Working Principles, Opportunities, and Challenges *Small Methods* 1900026

[20] Galvez N, Fernandez B, Sanchez P, Cuesta R, Ceolin M, Clemente-Leon M, Trasobares S, Lopez-Haro M, Calvino J J, Stephan O and Dominguez-Vera J M 2008 Comparative structural and chemical studies of ferritin cores with gradual removal of their iron contents *J. Am. Chem. Soc.* **130** 8062–8

[21] Wang W, Knovich M and Coffman L 2010 Serum ferritin: Past, present and future *Biochim. Biophys. ...* **1800** 760–9

[22] Massover W H 1993 Ultrastructure of ferritin and apoferritin: A review *Micron* **24** 389–437

[23] Alkhateeb A A and Connor J R 2010 Nuclear ferritin: A new role for ferritin in cell biology *Biochim. Biophys. Acta - Gen. Subj.* **1800** 793–7

[24] Arosio P and Levi S 2010 Cytosolic and mitochondrial ferritins in the regulation of cellular iron homeostasis and oxidative damage *Biochim. Biophys. Acta - Gen. Subj.* **1800** 783–92

[25] Hintze K J and Theil E C 2006 Cellular regulation and molecular interactions of the ferritins *Cell. Mol. Life Sci.* **63** 591–600

[26] Bou-Abdallah F 2010 The iron redox and hydrolysis chemistry of the ferritins *Biochim. Biophys. Acta - Gen. Subj.* **1800** 719–31

[27] Watt R K, Hilton R J and Graff D M 2010 Oxido-reduction is not the only mechanism allowing ions to traverse the ferritin protein shell *Biochim. Biophys. Acta - Gen. Subj.* **1800** 745–59

[28] Knovich M A, Storey J A, Coffman L G, Torti S V. and Torti F M 2009 Ferritin for the clinician *Blood Rev.* **23** 95–104

[29] Carmona F, Palacios ??scar, G??lvez N, Cuesta R, Atrian S, Capdevila M and Dom??nguez-Vera J M 2013 Ferritin iron uptake and release in the presence of metals and metalloproteins: Chemical implications in the brain *Coord. Chem. Rev.* **257** 2752–64

[30] Quintana C and Gutiérrez L 2010 Could a dysfunction of ferritin be a determinant factor in the aetiology of some neurodegenerative diseases? *Biochim. Biophys. Acta - Gen. Subj.* **1800** 770–82

[31] Harrison P M 1986 The structure and function of ferritin *Biochem. Educ.* **14**

[32] Banyard S H, Stammers D K and Harrison P M 1978 Electron density map of apoferritin at 2.8-Å resolution *Nature* **271** 282–4

[33] Bou-Abdallah F, Flint N, Wilkinson T, Salim S, Srivastava A K, Poli M, Arosio P and Melman A 2019 Ferritin exhibits Michaelis–Menten behavior with oxygen but not with iron during iron oxidation and core mineralization *Metallomics* **11** 774

[34] Takahashi T and Kuyucak S 2003 Functional properties of threefold and fourfold channels in ferritin deduced from electrostatic calculations *Biophys. J.* **84** 2256–63

[35] Douglas T and Ripoll D R 1998 Calculated electrostatic gradients in recombinant human H-chain ferritin. *Protein Sci.* **7** 1083–91

[36] Theil E C, Liu X S and Matzapetakis M 2010 Ferritin. Biomineralization of Iron *Biomineralization: From Nature to Application* vol 4 pp 327–41

[37] Liu X and Theil E C 2004 Ferritin reactions: direct identification of the site for the diferric peroxide reaction intermediate. *Proc. Natl. Acad. Sci. U. S. A.* **101** 8557–62

[38] Macara I G, Hoy T G and Harrison P M 1972 The

formation of ferritin from apoferritin. Kinetics and Mechanism of Iron untake *Biochem. J.* **126** 151–62

[39] Pozzi C, Ciambellotti S, Bernacchioni C, Di Pisa F, Mangani S and Turano P 2017 Chemistry at the protein–mineral interface in L-ferritin assists the assembly of a functional (μ 3 -oxo)Tris[(μ 2 -peroxo)] triiron(III) cluster *Proc. Natl. Acad. Sci.* **114** 2580–5

[40] Cheng Y G and Dennis N C 1991 Role of Phosphate in Initial Iron Deposition in Apoferritin *Biochemistry* **30** 2947–53

[41] Harrison P M, Hoy T G, Macara I G and Hoare R J 2015 Ferritin iron uptake and release. Structure–function relationships *Biochem. J.* **143** 445–51

[42] Trefry A and Harrison P M 1978 Incorporation and release of inorganic phosphate in horse spleen ferritin *Biochem. J.* **171** 313–20

[43] Chasteen N D and Theil E C 1982 Iron binding by horse spleen apoferritin. A vanadyl(IV) EPR spin probe study *J. Biol. Chem.* **257** 7672–7

[44] Hanna P M, Chasteen N D, Rottman G A and Aisen P 1991 Iron Binding to Horse Spleen Apoferritin: A Vanadyl ENDOR Spin Probe Study *Biochemistry* **30** 9210–6

[45] Bauminger E R, Harrison P M, Hechel D, Nowik I and Treffry A 1991 Iron (III) can be transferred between ferritin molecules *Proc. R. Soc. B Biol. Sci.* **244** 211–7

[46] Chen-yui Yang, Adrian Meagher,Boi Hanh Huynh, Dale E. Sayers and E C T 1987 Iron(III) clusters bound to horse spleen apoferritin: an x-ray absorption and Moessbauer spectroscopy study that shows that iron nuclei can form on the protein *Biochemistry* **26** 497–503

[47] Harrison P M, Treffry A and Lilley T H 1986 Ferritin as an iron-storage protein: mechanisms of iron uptake *J. Inorg. Biochem.* **27** 287–93

[48] Mobarra N, Shanaki M, Ehteram H, Nasiri H, Sahmani M, Saeidi M, Goudarzi M, Pourkarim H and Azad M 2016 A review on iron chelators in treatment of iron overload syndromes *Int. J. Hematol. Stem Cell Res.* **10** 239–47

[49] Vichinsky E P 2002 Current issues with blood transfusions in sickle cell disease *Semin. Hematol.* **38** 14–22

[50] Yasmin S, Andrews S C, Moore G R and Le Brun N E 2011 A new role for heme, facilitating release of iron from the bacterioferritin iron biomineral *J. Biol. Chem.* **286** 3473–83

[51] Truty J, Malpe R and Linder M C 2001 Iron Prevents Ferritin Turnover in Hepatic Cells *J. Biol. Chem.* **276** 48775–80

[52] Kurz T 2007 Can Lipofuscin Accumulation Be Prevented? *Rejuvenation Res.* **11** 441–3

[53] Galvez N, Ruiz B, Cuesta R, Colacio E and Dominguez-Vera J M 2005 Release of iron from ferritin by aceto- and benzohydroxamic acids *Inorg. Chem.* **44** 2706–9

[54] Joo M S, Tourillon G, Sayers D E and Theil E C 1990 Rapid reduction of iron in horse spleen ferritin by thioglycolic acid measured by dispersive X-ray absorption spectroscopy *Biol. Met.* **3** 171–5

[55] Sirivech S, Frieden E and Osaki S 2015 The release of iron from horse spleen ferritin by reduced flavins *Biochem. J.* **143** 311–5

[56] Shi H, Bencze K Z, Stemmler T L and Philpott C C 2008 A cytosolic iron chaperone that delivers iron to ferritin. *Science* **320** 1207–10

[57] Tosha T, Behera R K, Ng H L, Bhattasali O, Alber T and Theil E C 2012 Ferritin protein nanocage ion channels: Gating by N-terminal extensions *J. Biol. Chem.* **287** 13016–25

[58] Watt G D, McDonald J W, Chiu C H and Reddy K R N 1993 Further characterization of the redox and spectroscopic properties of azotobacter vinelandii ferritin *J. Inorg. Biochem.* **51** 745–58

[59] Watt G D, Frankel R B and Papaefthymiou G C 2006 Reduction of mammalian ferritin. *Proc. Natl. Acad. Sci.* **82** 3640–3

[60] Kourkoutis L F, Plitzko J M and Baumeister W 2012 Electron Microscopy of Biological Materials at the Nanometer Scale *Annu. Rev. Mater. Res.* **42** 33–58

[61] Anon 1972 An ultrastructural staining method for enhancing the size and electron opacity of ferritin in thin sections *J. Histochem. Cytochem.* **20** 225–9

[62] Heuser J E 1983 Procedure for freeze-drying molecules adsorbed to mica flakes *J. Mol. Biol.* **169** 155–95

[63] Taylor K A and Glaeser R M 1976 Electron Microscopy of Frozen Hydrated Biological Specimens at the level of atomic resolution is a major *J. Ultrastruct. Res.* **55** 448–56

[64] Massover, W.H., Adrian M 1986 Ultrastructure of vitrified (frozen-hydrated) ferritin and apoferritin *Porc. XIth Cong. on Electron Microscopy* pp 2427–2428

[65] Thompson R F, Walker M, Siebert C A, Muench S P and Ranson N A 2016 An introduction to sample preparation and imaging by cryo-electron microscopy for structural biology *Methods* **100** 3–15

[66] Fan X, Zhao L, Liu C, Zhang J C, Fan K, Yan X, Peng H L, Lei J and Wang H W 2017 Near-Atomic Resolution Structure Determination in Over-Focus with Volta Phase Plate by Cs-Corrected Cryo-EM *Structure* **25** 1623-1630.e3

[67] Schultz P 1988 Cryo-electron microscopy of vitrified specimens *Q. Rev. Biophys.* **21** 129–228

[68] Klint D, Karlsson G and Bovin J O 1999 Cryo-TEM snapshots of ferritin adsorbed on small zeolite crystals *Angew. Chemie - Int. Ed.* **38** 2560–2

[69] Halle B 2004 Biomolecular cryocrystallography: Structural changes during flash-cooling *Proc. Natl. Acad. Sci.* **101** 4793–8

[70] Levy Y and Onuchic J N 2006 Water Mediation in Protein Folding and Molecular Recognition *Annual*

Review of Biophysics and Biomolecular Structure vol 35 pp 389–415

[71] Jonge N D and F M R 2011 Electron microscopy of specimens in liquid *Nat. Nanotechnol.* **6**

[72] Peckys D B B, Mazur P, Gould K L L, De Jonge N, de Jonge N and De Jonge N 2011 Fully hydrated yeast cells imaged with electron microscopy *Biophys. J.* **100** 2522–9

[73] Evans J E and Browning N D 2013 Enabling direct nanoscale observations of biological reactions with dynamic TEM *J. Electron Microsc. (Tokyo).* **62** 147–56

[74] Textor M and De Jonge N 2018 Strategies for Preparing Graphene Liquid Cells for Transmission Electron Microscopy *Nano Lett.* **18** 3313–21

[75] Wang C, Shokuhfar T and Klie R F 2016 Precise In Situ Modulation of Local Liquid Chemistry via Electron Irradiation in Nanoreactors Based on Graphene Liquid Cells *Adv. Mater.* **28** 7716–22

[76] Cho H, Jones M R, Nguyen S C, Hauwiller M R, Zettl A and Alivisatos A P 2017 The Use of Graphene and Its Derivatives for Liquid-Phase Transmission Electron Microscopy of Radiation-Sensitive Specimens *Nano Lett.* **17** 414–20

[77] Chen Q, Smith J M, Park J, Kim K, Ho D, Rasool H I, Zettl A and Alivisatos A P 2013 3D motion of DNA-Au nanoconjugates in graphene liquid cell electron microscopy *Nano Lett.* **13** 4556–61

[78] Farrant J L 1954 An electron microscopic study of ferritin *Biochim. Biophys. Acta* **13** 569–76

[79] Muir A R 1960 The molecular structure of isolated and intracellular ferritin *Q. J. Exp. Physiol. Cogn. Med. Sci.* **45** 192–201

[80] KERR D N and MUIR A R 1960 A demonstration of the structure and disposition of ferritin in the human liver cell. *J. Ultrastruct. Res.* **3** 313–9

[81] A.R. Muir 1960 The Molecular Structure of Isolated and Intrecellular Ferritin

[82] Towe K M and Bradley W F 1967 Mineralogical constitution of colloidal “hydrous ferric oxides” *J. Colloid Interface Sci.* **24** 384–92

[83] Massover W H and Cowley J M 1973 The Ultrastructure of Ferritin Macromolecules. The Lattice Structure of the Core Crystallites *Proc. Natl. Acad. Sci.* **70** 3847–51

[84] Haggis G H 1965 The iron oxide core of the ferritin molecule *J. Mol. Biol.* **14** 598–602

[85] Haydon G B, Division E P and Medical P A 1969 Visualization of substructure in ferritin molecules : an artifact *J. Microsc.* **89** 251–61

[86] Haydon G B 1970 Further observations concerning the substance of ferritin molecules *J. Microsc.* **91** 65–6

[87] Towe K M 1969 Substructure in the iron core of ferritin molecules *J. Microsc.* **90** 279–81

[88] TANAKA N and MIHAMA K 2017 Observations of Ferritin Particles by Using BeO Supporting Films *J. Electron Microsc. (Tokyo).* **26** 75–85

[89] Hahn M and Baumeister W 1974 High resolution negative staining of ferritin molecules on vermiculite single crystal supports *BBA - Protein Struct.* **371** 267–74

[90] Crewe A V and Wall J 1970 A scanning microscope with 5 Å resolution *J. Mol. Biol.* **48** 375–93

[91] Ohtsuki M, Isaacson M S and Crewe a V 1979 Dark field imaging of biological macromolecules with the scanning transmission electron microscope. *Proc. Natl. Acad. Sci. U. S. A.* **76** 1228–32

[92] Treacy M, Howie A and Wilson C J 2002 *Philosophical magazine. A.* vol 38 (Taylor & Francis)

[93] Pan Y H, Sader K, Powell J J, Bleloch A, Gass M, Trinick J, Warley A, Li A, Brydson R and Brown A 2009 3D morphology of the human hepatic ferritin mineral core: New evidence for a subunit structure revealed by single particle analysis of HAADF-STEM images *J. Struct. Biol.* **166** 22–31

[94] Fischbach F A, Harrison P M and Hoy T G 1969 The structural relationship between ferritin protein and its mineral core. *J. Mol. Biol.* **39** 235–8

[95] Ford G C, Harrison P M, Rice D W, Smith J M A, Treffry A, White J L and Yariv J 1984 Ferritin: Design and Formation of an Iron-Storage Molecule *Philos. Trans. R. Soc. B Biol. Sci.* **304** 551–65

[96] López-Castro J D, Delgado J J, Perez-Omil J A, Gálvez N, Cuesta R, Watt R K and Domínguez-Vera J M 2012 A new approach to the ferritin iron core growth: influence of the H/L ratio on the core shape. *Dalton Trans.* **41** 1320–4

[97] Pan Y-H, Brown A, Sader K, Brydson R, Gass M and Bleloch A 2008 Quantification of absolute iron content in mineral cores of cytosolic ferritin molecules in human liver *Mater. Sci. Technol.* **24** 689–94

[98] Jian N, Dowle M, Horniblow R D, Tselepis C and Palmer R E 2016 Morphology of the ferritin iron core by aberration corrected scanning transmission electron microscopy *Nanotechnology* **27**

[99] Walls M G, Cao C, Yu-Zhang K, Li J, Che R and Pan Y 2013 Identification of ferrous-ferric Fe3O4 nanoparticles in recombinant human ferritin cages. *Microsc. Microanal.* **19** 835–41

[100] Drits V 1993 Structural Model for Ferrihydrite *Clay Miner.* **28** 185–207

[101] Michel F M, Ehm L, Antao S M, Lee P L, Chupas P J, Liu G, Strongin D R, Schoonen M A A, Phillips B L and Parise J B 2007 The structure of ferrihydrite, a nanocrystalline material *Science (80-.).* **316** 1726–9

[102] Michel F M, Hosein H A, Hausner D B, Debnath S, Parise J B and Strongin D R 2010 Reactivity of ferritin and the structure of ferritin-derived ferrihydrite *Biochim. Biophys. Acta - Gen. Subj.* **1800** 871–85

[103] Jambor J L and Dutrizac J E 1998 Occurrence and Constitution of Natural and Synthetic Ferrihydrite, a Widespread Iron Oxyhydroxide *Chem. Rev.* **98**

2549–86

[104] Janney D E, Cowley J M and Buseck P R 2000 Transmission electron microscopy of synthetic 2- and 6-line ferrihydrite *Clays Clay Miner.* **48** 111–9

[105] Mann S, Bannister J V and Williams R J 1986 Structure and composition of ferritin cores isolated from human spleen, limpet (Patella vulgata) hemolymph and bacterial (Pseudomonas aeruginosa) cells [published erratum appears in J Mol Biol 1986 Jul 5;190(1):139] *J Mol Biol* **188** 225–32

[106] Weiser B H and Milligan W . 1940 Electron Diffraction Study of Hydrous Oxides amorphous to X-Rays *J. Phys. Chem.* **44** 1081

[107] Towe K M and Bradley W F 1967 Mineralogical constitution of colloidal "hydrous ferric oxides" *J. Colloid Interface Sci.* **24** 384–92

[108] Quintana C, Bonnet N, Jeantet A Y and Chemelle P 1987 Crystallographic study of the ferritin molecule: new results obtained from natural crystals in situ (mollusc oocyte) and from isolated molecules (horse spleen) *Biol. Cell* **59** 247–54

[109] Towe K M and Moench T T 1981 Electron-optical characterization of bacterial magnetite *Earth Planet. Sci. Lett.* **52** 213–20

[110] Mann S, Williams J M, Treffry A and Harrison P M 1987 Reconstituted and native iron-cores of bacterioferritin and ferritin *J. Mol. Biol.* **198** 405–16

[111] Brady G W, Kurkjian C R, Lyden E F X, Robin M B, Saltman P, Spiro T and Terzis A 1968 The Structure of an Iron Core Analog of Ferritin *Biochemistry* **7** 2185–92

[112] Heald S M, Bunker B, Holt E M and Holt S L 1979 Structure of the Iron-Containing Core in Ferritin by the Extended X-ray Absorption Fine Structure Technique *J. Am. Chem. Soc.* **101** 67–73

[113] Hoy T G, Harrison P M and Shabbir M 1974 Uptake and release of ferritin iron. Surface effects and exchange within the crystalline core. *Biochem. J.* **139** 603–7

[114] Watt G D, Jacobs D and Frankel R B 1988 Redox Reactivity of Bacterial and Mammalian Ferritin: Is Reductant Entry into the Ferritin Interior a Necessary Step for iron Release? *Proc. Natl. Acad. Sci. U. S. A.* **85** 7457–61

[115] Quintana C, Lancin M, Marhic C, Pérez M, Martin-Benito J, Avila J and Carrascosa J L 2000 Initial studies with high resolution TEM and electron energy loss spectroscopy studies of ferritin cores extracted from brains of patients with progressive supranuclear palsy and Alzheimer disease. *Cell. Mol. Biol.* **46** 807–20

[116] Quintana C, Cowley J M and Marhic C 2004 Electron nanodiffraction and high-resolution electron microscopy studies of the structure and composition of physiological and pathological ferritin *J. Struct. Biol.* **147** 166–78

[117] Quintana C, Bellefqih S, Laval J Y, Guerquin-Kern J L, Wu T D, Avila J, Ferrer I, Arranz R and Patiño C 2006 Study of the localization of iron, ferritin, and hemosiderin in Alzheimer's disease hippocampus by analytical microscopy at the subcellular level *J. Struct. Biol.* **153** 42–54

[118] Collingwood J F, Chong R K K, Kasama T, Cervera-Gontard L, Dunin-Borkowski R E, Perry G, Pósfai M, Siedlak S L, Simpson E T, Smith M a and Dobson J 2008 Three-dimensional tomographic imaging and characterization of iron compounds within Alzheimer's plaque core material. *J. Alzheimers. Dis.* **14** 235–45

[119] Pan Y H, Vaughan G, Brydson R, Bleloch A, Gass M, Sader K and Brown A 2010 Electron-beam-induced reduction of Fe3+ in iron phosphate dihydrate, ferrihydrite, haemosiderin and ferritin as revealed by electron energy-loss spectroscopy *Ultramicroscopy* **110** 1020–32

[120] Calvert C C, Brown A and Brydson R 2005 Determination of the local chemistry of iron in inorganic and organic materials *J. Electron Spectros. Relat. Phenomena* **143** 173–87

[121] Pan Y, Brown A, Brydson R, Warley A, Li A and Powell J 2006 Electron beam damage studies of synthetic 6-line ferrihydrite and ferritin molecule cores within a human liver biopsy *Micron* **37** 403–11

[122] Yuk J M, Park J, Ercius P, Kim K, Hellebusch D J, Crommie M F, Lee J Y, Zettl A, Alivisatos A P and Yuk Min Jong, Park, Jungwon, Ercius, Peter, Kwanpyo, Kim, Hellebusch J Daniel, Crommie F Michael, Lee Yong Jeong, Zettl A A A P 2012 High-Resolution Em of Colloidal Nanocrystal Growth Using Graphene Liquid Cells *Science (80-.).* **336** 61–4

[123] Soltau H, Sagawa R, Ryll H, Nellist P D, MacLaren I, Banba H, Simson M, Kondo Y, Yang H and Jones L 2015 4D STEM: High efficiency phase contrast imaging using a fast pixelated detector *J. Phys. Conf. Ser.* **644** 012032

[124] Ophus C, Ercius P, Sarahan M, Czarnik C and Ciston J 2014 Recording and using 4D-STEM datasets in materials science *Microscopy and Microanalysis* vol 20 (Springer) pp 62–3

[125] Fang S, Wen Y, Allen C S, Ophus C, Han G G D, Kirkland A I, Kaxiras E and Warner J H 2019 Atomic electrostatic maps of 1D channels in 2D semiconductors using 4D scanning transmission electron microscopy *Nat. Commun.* **10**

[126] van Aken P A, Suyolcu Y E, Wang Y, Sigle W, Srot V, Salzberger U and Hahn K 2018 Correcting the linear and nonlinear distortions for atomically resolved STEM spectrum and diffraction imaging *Microscopy* **67** i114–22

[127] Miao J, Ercius P and Billinge S J L 2016 Atomic electron tomography: 3D structures without crystals *Science (80-.).* **353**

[128] Carenco S, Moldovan S, Roiban L, Florea I, Portehault D, Vallé K, Belleville P, Boissière C, Rozes L, Mézailles N, Drillon M, Sanchez C and

Ersen O 2016 The core contribution of transmission electron microscopy to functional nanomaterials engineering *Nanoscale* **8** 1260–79

[129] Chen C-C, Marks L D, Scott M C, Ercius P, Yang Y, Ramezani-Dakhel H, Xu R, Theis W, Heinz H, Sawaya M R, Miao J, Ophus C, Wu L and Bartels M 2015 Three-dimensional coordinates of individual atoms in materials revealed by electron tomography *Nat. Mater.* **14** 1099–103

[130] Chen C-C, Regan B C, Scott M C, Marks L D, Huang Y, Chiu C-Y, Miao J, Zhu C and White E R 2013 Three-dimensional imaging of dislocations in a nanoparticle at atomic resolution *Nature* **496** 74–7

[131] Chasteen N D and Harrison P M 1999 Mineralization in ferritin: an efficient means of iron storage. *J. Struct. Biol.* **126** 182–94

[132] Cho K J, Shin H J, Lee J H, Kim K H J, Park S S S S, Lee Y, Lee C, Park S S S S and Kim K H J 2009 The Crystal Structure of Ferritin from Helicobacter pylori Reveals Unusual Conformational Changes for Iron Uptake *J. Mol. Biol.* **390** 83–98

[133] Picher M, Mazzucco S, Blankenship S and Sharma R 2015 Vibrational and optical spectroscopies integrated with environmental transmission electron microscopy *Ultramicroscopy* **150** 10–5

[134] Bernacchioni C, Ghini V, Theil E C and Turano P 2016 Modulating the permeability of ferritin channels *RSC Adv.* **6** 21219–27

[135] Costa T R D, Ignatiou A and Orlova E V. 2017 Structural analysis of protein complexes by cryo electron microscopy *Methods in Molecular Biology* vol 1615 (Humana Press, New York, NY) pp 377–413

[136] Narayanan S, Firlar E, Golam Rasul Md, Foroozan T, Farajpour N,Covnot L, Shahbazian-Yassar R, and Shokuhfar T 2019 On the Structure and Chemistry of Iron Oxide Cores in Human Heart and Human Spleen Ferritins using Graphene Liquid Cell Electron Microscopy, Nanoscale (Under Review)